below the DSCR edge when it corresponds to a minimum of $\partial S/\partial k_z$.

These two effects are closely related to the resonant launching of the Gantmakher excitations by the dispersive waves.

ACKNOWLEDGMENTS

It is a great pleasure to thank Dr. R. L. Powell for sending us his computed copper Fermi surface, and C. Laroche for technical assistance in sample preparation and experiments.

PHYSICAL REVIEW B VOLUME 1, NUMBER 4 15 FEBRUARY 1970

Third-Order Elastic Constants of Zinc*

K. D. Swartz† and C. Elbaum
Department of Physics, Brown University, Providence, Rhode Island 02912

(Received 4 August,1969)

The complete set of ten third-order elastic constants of zinc was determined from measurements of the hydrostatic and uniaxial stress dependence of ultrasonic velocity. The experiments were carried out using the two-specimen interferometric method on appropriately oriented single crystals of zinc. The magnitudes of C_{222} and C_{111} are largest, followed by C_{333} which is less than one-third of C_{222}, whereas C_{144} is the smallest of all. All the constants except C_{155} are negative. The "macroscopic" values of the Grüneisen γ for zinc are evaluated.

INTRODUCTION

CRYSTAL anharmonicity determines or affects various properties of solids, for example, thermal expansion, thermal conductivity, temperature dependence of elastic constants, and attenuation of high-frequency waves. The theoretical treatment of crystal anharmonicity usually involves an expansion of the strain energy of a crystal in terms of finite strains. The coefficients of terms of a given order in this expansion are conveniently defined as the corresponding-order elastic constants. Alternatively second-, third-, and higher-order elastic constants can be defined as the second, third, and higher derivatives of the free energy (isothermal constants) or of the internal energy (adiabatic constants) of the crystal with respect to finite strains. From the knowledge of higher-order elastic constants it is possible, in some cases, to estimate the relative importance of various contributions to the interatomic potential as well as to determine the general form of this potential.

The present work is concerned with the determination of the third-order elastic constants (TOEC) of zinc. As far as the authors are aware, this is the first report of a complete set of TOEC for a metal with the hexagonal-close-packed crystal structure.

The TOEC were obtained from measurements of the hydrostatic and uniaxial stress dependence of sound velocity in single crystals. In the case of solids containing mobile dislocations, such measurements must be carried out in a manner such as to eliminate or subtract the added effects of dislocations. The dependence of the attenuation of the propagating wave on amplitude and on static stress is a sensitive indicator of dislocation effects.[1] This method was used, therefore, to ascertain whether dislocations were affecting the measurements. In the present study all propagation modes having a shear component of stress in the (0001) plane were found to be sensitive to dislocations when zinc crystals of nominal purity 99.999% were used. No such sensitivity was found, however, in zinc crystals containing 0.5% (atomic) aluminum. For all the other propagation modes used, dislocation effects were not detected in either the high-purity zinc or the zinc containing the aluminum. As is shown later, the TOEC obtained on the two types of crystals were the same, within the experimental uncertainty of the measurements.

EXPERIMENTAL PROCEDURE AND RESULTS

The zinc single crystals were grown from the melt with predetermined orientation. Two sets of single crystals were prepared, one of 99.999% pure zinc, the other using the same starting material with the addition of 0.5% (atomic) aluminum to the melt. Precautions were taken to insure uniformity of composition for the second set of samples. All the specimens were in the shape of parallelepipeds; those of higher purity had the approximate dimensions 1.5×1.5×2.0 cm, the ones of lower purity had the approximate dimensions 0.9 ×1.1×1.4 cm. They were prepared from the respective single crystals by cutting and planing on a spark

---

* Work supported in part by the National Science Foundation.

† Summer visitor under National Science Foundation grant. Permanent address: Department of Physics W.P.I., Worcester, Mass. 01609.

[1] R. Truell, C. Elbaum, and B. B. Chick, *Ultrasonic Methods in Solid State Physics* (Academic Press Inc., New York, 1969).

cutting machine and were given a final hand polishing to obtain the same dimensions for equivalent crystallographic directions. The orientations were checked by Laue x-ray diffraction patterns; the faces of the specimens were thus found to be within 1° normal to the directions $[0001]$, $[\bar{1}\bar{1}20]$, $[1\bar{1}00]$. It is estimated that after polishing, the dimensions of each pair of equivalent samples were the same to within $\pm 2 \times 10^{-4}$ cm.

As a preliminary check, measurements of the adiabatic second-order elastic constants were made by means of the usual "pulse-echo technique."[1] These results were found to be the same as the results of Alers and Neighbours within ±0.5%. Since the absolute accuracy of the measuring equipment used here was less than that of Alers and Neighbours,[2] we used their values for the second-order elastic constants on all subsequent occasions where such constants were needed.

The technique used for measuring the temperature and pressure dependence of the wave velocities was the two-specimen interferometric method, which has been described elsewhere.[3] The only major modification of the apparatus design used in the present investigation was the incorporation of a signal divider for the signal coming from the signal generator. This signal divider allowed one to make the signal levels from the two specimens equal. It was then observed that the interference pattern became sharper, i.e., the height of the null echo approached zero better than without the signal divider. This adjustment was always made before the experimental run commenced. The temperature difference between the two specimens was monitored by means of iron-constantan thermocouples. Those thermocouples were calibrated against a platinum resistance thermometer in the range from 10 to 25°C. An ultrasonic frequency of 10 MHz was used throughout this study.

When a velocity difference ΔW exists between two specimens, an interference results when the two waves are recombined, and the velocity difference is given by[4]

$$\frac{\Delta W}{W_0}=\frac{(2j-1)}{n}\,\frac{1}{2ft_0}, \qquad (1)$$

where j is the interference node number, n is the echo number, f is the frequency, and t_0 is the round-trip echo time. Here we use the concept of a natural velocity, $W_0=2L_0/t_0$, with L_0 being the ultrasonic pathlength at the reference temperature in the absence of an applied stress, and t_0 having the same meaning as above. Changes in velocity difference ΔW with changing temperature are essentially equivalent to changes in the quantity $(2j-1)/n$ with temperature. The temperature coefficient of the natural velocity, $\beta'=\partial \ln W/\partial T$, is found by plotting $(2j-1)/n$ versus the difference in temperature, ΔT, and multiplying the slope of this graph by $1/2ft_0$. In order to convert these temperature coefficients to the corresponding temperature coefficients of the elastic constants the following relationship is used:

$$\partial \ln C_{ij}/\partial T=-(\alpha_{11}+2\alpha_{33})+2(\alpha_{ij})+2\beta', \qquad (2)$$

where α_{11} is the thermal expansion coefficient parallel to the c axis, α_{33} is the thermal expansion coefficient perpendicular to the c axis, α_{ij} is the thermal-expansion coefficient appropriate to the direction along which the ultrasonic wave is traveling, β' is the temperature coefficient of the natural velocity which has been measured, and C_{ij} is the appropriate combination of second-order elastic constants which relate to the ultrasonic wave being propagated.

TABLE I. Temperature coefficients of four second-order elastic constants of Zn around room temperature [$\partial C_{ij}/\partial T$ in units of 10^8 dyn/(cm^2 °C)].

	Present	Alers and Neighbours
$\partial C_{11}/\partial T$	-6.61 ± 0.17	-6.65
$\partial C_{44}/\partial T$	-2.89 ± 0.10	-2.82
$\partial C_{33}/\partial T$	-2.02 ± 0.08	-1.71
$\partial C'/\partial T=\frac{1}{2}\partial(C_{11}-C_{12})/\partial T$	-3.40 ± 0.11	-3.39

In the case of zinc, the two-specimen method can only give the temperature coefficients of four of the five second-order elastic constants which appear in the wave velocities with pure modes. These are C_{11}, C_{12}, C_{44}, and C_{33}. Furthermore, there is no consistency check on the constant C_{33} as it may be obtained only by propagation of a longitudinal wave along the c axis. There are enough distinct modes for consistency checks on each of the three other constants, however. The thermal-expansion coefficients of zinc determined by Collins and White[5] were used to relate the measured (β')'s with the temperature coefficients of the elastic constants. The results obtained in this study along with those of Alers and Neighbours,[2] are shown in Table I. The values labeled "Alers and Neighbours" are calculated from their tables of elastic constants versus temperature in the region around room temperature. The values $\partial C_{ij}/\partial T$ obtained here are based on measurements over a small interval of temperature (10° or less), near room temperature. They are, therefore, expected to be more accurate, at this temperature, than values obtained by Alers and Neighbours over an interval of 100°, spanning room temperature. It is seen, however, that the two sets of measurements show very good agreement for C_{11}, C', C_{44}, and fairly good agreement for C_{33}.

---

[2] G. A. Alers and J. R. Neighbours, J. Phys. Chem. Solid **7**, 58 (1958).

[3] Y. Hiki and A. V. Granato, Phys. Rev. **36**, 2504 (1965).

[4] R. F. Espinola and P. C. Waterman, J. Appl. Phys. **29**, 718 (1958).

[5] J. G. Collins and G. K. White, in *Progress in Low Temperature Physics*, edited by C. J. Gorter (North-Holland Publishing Co., Amsterdam, 1964), Vol. 4, p. 450.

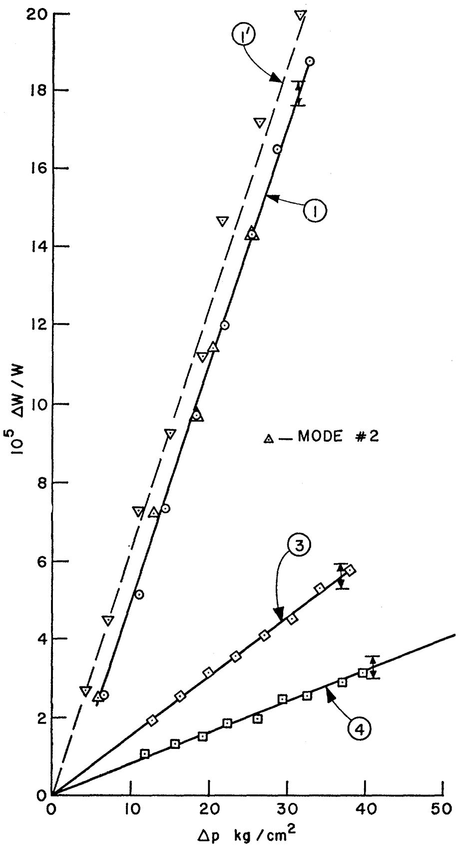

FIG. 1. Natural velocity change $\Delta W/W$ as a function of hydrostatic stress in zinc. The numbers refer to the modes specified in Table II. Note that mode (1) (circles) and mode (2) (triangles) superimpose, thus only one line has been drawn for both sets of points.

The stress measurements procede in the following fashion. A null in the interference pattern is established by maintaining a temperature difference between the samples. When the stress, either hydrostatic or uniaxial, is applied the null shifts by a small amount. The original null condition is then reestablished by changing the temperature of the sample which is not being stressed. The hydrostatic stress is obtained by means of compressed nitrogen gas (from a tank). The pressure is read on a U. S. Gauge Co. pressure gauge which is accurate to about 1.5%. The uniaxial stress is supplied by a hydraulic press which was calibrated against dead loads. The specimen was compressed between two steel plates, one of which was connected to the press by a ball-and-socket arrangement in an effort to minimize misalignments. Indium shims were inserted between the specimen and the pressure plates.

TABLE II. Directions of static stress, M, of wave propagation, N, and of wave polarization U, along with the appropriate elastic constants.[a]

M	N	U	$(\rho_0 w^2)_{P=0}$	Correlation to Brugger's formula for $(\rho_0 w^2)'$
1. Hydrostatic	[001]	[001]	C_{33}	$M_0\alpha L$
2. Hydrostatic	[001]	[100] or [010]	C_{44}	$M_0\alpha T_1$ or $M_0\alpha T_2$
3. Hydrostatic	[100]	[100]	C_{11}	$M_0\gamma L$
4. Hydrostatic	[100]	[010]	$\frac{1}{2}(C_{11}-C_{12})$	$M_0\gamma T_2$
5. Hydrostatic	[100]	[001]	C_{44}	$M_0\gamma T_3$
6. [001]	[100]	[100]	C_{11}	$M_3\gamma L$
7. [001]	[100]	[010]	$\frac{1}{2}(C_{11}-C_{12})$	$M_3\gamma T_2$
8. [010]	[001]	[010]	C_{44}	$M_2\alpha T_2$
9. [010]	[100]	[100]	C_{11}	$M_2\gamma L$
10. [010]	[100]	[010]	$\frac{1}{2}(C_{11}-C_{12})$	$M_2\gamma T_2$
11. [010]	[001]	[100]	C_{44}	$M_2\alpha T_1$
12. [010]	[001]	[001]	C_{33}	$M_2\alpha L$

[a] M_0, α, L, γ, T_1, T_2, T_3, are explained in Ref. 6.

Brugger's[6] formulation is used to relate the change in natural velocity with stress to TOEC. This is done by relating the change in temperature difference for the null condition with stress to the change in natural velocity in the manner shown below:

$$(\rho_0 w^2)'_{P=0}=2(\rho_0 w^2)_{P=0}\frac{\Delta W}{W\Delta T}\,\delta\frac{\Delta T}{\Delta P}\bigg|_{P=0}, \qquad (3)$$

where $(\rho_0 w^2)'$ is the pressure derivative of the modified elastic constant as defined by Thurston and Brugger,[7]

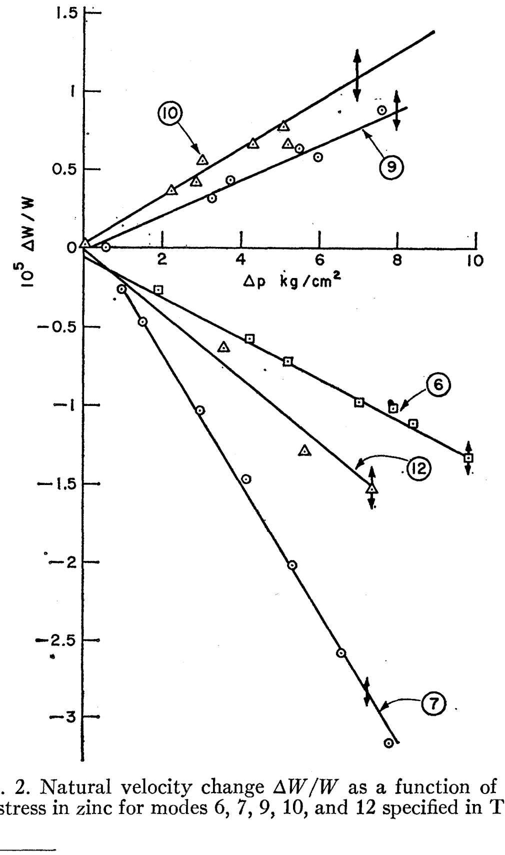

FIG. 2. Natural velocity change $\Delta W/W$ as a function of uniaxial stress in zinc for modes 6, 7, 9, 10, and 12 specified in Table II.

---

[6] K. Brugger, J. Appl. Phys. 36, 767 (1965).

[7] R. N. Thurston and K. Brugger, Phys. Rev. 133, A1604 (1964).

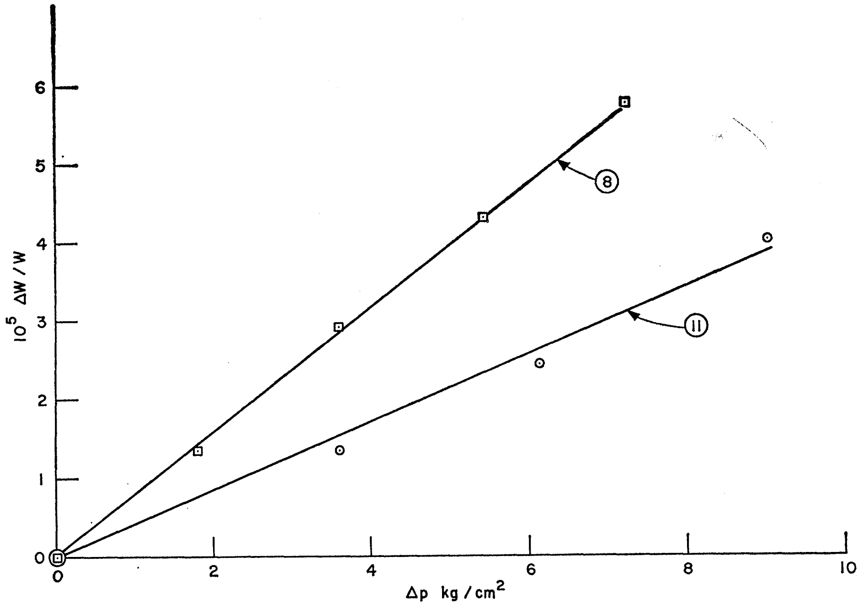

FIG. 3. Natural velocity change $\Delta W/W$ as a function of uniaxial stress in zinc for modes 8 and 11 specified in Table II.

$\delta\Delta T=\Delta T|_{P=P}-\Delta T|_{P=0}$, $\Delta W/W\Delta T$ is the measured temperature coefficient of natural velocity, and $(\rho_0 w^2)$ is the elastic constant appropriate to the mode of ultrasonic propagation. In Table II we give the directions of static stress, M, of wave propagation, N, and of wave polarization, U, along with the appropriate elastic constants. The coordinate axes used are those specified by the IRE standards[8] and the elastic constants used are based on the definitions of Brugger.[6] The plots of $\Delta W/W$ versus ΔP for the hydrostatic stress measurements are shown in Fig. 1. The plots of $\Delta W/W$ versus ΔP for the uniaxial stress measurements are shown in Figs. 2 and 3. The arrows denote the uncertainty in each measurement. Note that the modes involving C_{44} are plotted in Fig. 3. These modes were measured on the "impure" samples, because dislocation effects present in the pure samples made it difficult to obtain reliable values for the stress dependence of the natural velocity. The consistency of results obtained on the two sets of samples for the mode involving C_{33} was checked and is shown by the curves labeled (1) and (1′) in Fig. 1.

In Table III we give the equations necessary to evaluate the TOEC of zinc from the measured slopes. The numbers in line 1, correspond to the numbers in Table II. The coefficients of the TOEC were calculated from the adiabatic second-order elastic compliances of Alers and Neighbours.[2] This should not cause a significant discrepancy in the final results, even though Brugger's formulas call for isothermal compliances, since the correction from adiabatic to isothermal compliances is characteristically of the order of 1%.

The equations involving the TOEC are segregated in the following manner. C_{111}, C_{112}, C_{222}, C_{123}, and C_{113} occur only when the ultrasonic wave is propagated in the basal plane and is polarized in that plane. C_{133} and

TABLE III. Equations for evaluation for the TOEC of zinc. (In this table, one reads the equation horizontally, e.g., for line 1, the equation would read $1.329C_{333}+0.2974C_{133}=-10.382$.)

	C_{111}	C_{112}	C_{222}	C_{123}	C_{113}	C_{133}	C_{333}	C_{144}	C_{155}	C_{344}	M
1.	0	0	0	0	0	0.2974	1.329	0	0	0	−10.382
1′.[a]	0	0	0	0	0	0.2974	1.329	0	0	0	−10.93
2.[a]	0	0	0	0	0	0	0	0.1487	0.1487	1.329	− 5.53
3.	0.1487	0.1487	0	0	1.329	0	0	0	0	0	− 6.648
4.	0	−0.07435	0.07435	−0.6645	0.6645	0	0	0	0	0	− 2.123
5.[a]	0	0	0	0	0	0	0	0.1487	0.1487	1.329	− 4.856[b]
6.	−0.747	−0.747	0	0	2.283	0	0	0	0	0	8.141
7.	0	0.3735	−0.3735	−1.412	1.412	0	0	0	0	0	6.952
8.[a]	0	0	0	0	0	0	0	0.0547	0.841	−0.747	5.43
9.	0.0547	0.841	0	0	−0.747	0	0	0	0	0	− 4.058
10.	0.3432	−0.2239	−0.1692	0.3735	−0.3735	0	0	0	0	0	− 3.035
11.[a]	0	0	0	0	0	0	0	0.841	0.0547	−0.747	3.36
12.	0	0	0	0	0	0.8957	−0.747	0	0	0	2.243

[a] Values obtained from measurements carried out on the alloyed crystals.
[b] Questionable value.

---

[8] Proc. IRE **37**, 1378 (1949).

TABLE IV. TOEC of zinc obtained from ultrasonic waves in the basal plane. (C_{ijk} in units of 10^{12} dyn/cm^2.)

C_{111}	C_{112}	C_{222}	C_{123}	C_{113}	Weight
-17.31 ± 3.63	-5.08 ± 1.07	-22.00 ± 3.01	-3.15 ± 0.90	-2.87 ± 0.48	Unweighted
-17.56 ± 1.49	-4.40 ± 1.09	-24.14 ± 2.59	-2.14 ± 0.62	-2.68 ± 0.31	Weighted 4(3):1(6):1(9): 5(4):2(7):1(10)

C_{333} occur only when a longitudinal wave is propagated along the c axis. C_{144}, C_{155}, and C_{344} occur only when the ultrasonic mode involves the stress dependence of the elastic constant C_{44}. We further note from Table III that there are six independent relations among the five constants, C_{111}, C_{112}, C_{222}, C_{123}, and C_{113}. This allows for a check of the consistency of results. The constants C_{133} and C_{333} are checked by three measurements on two different sets of samples. The three constants C_{144}, C_{155}, C_{344} have no consistency check; they are all based on measurements involving the C_{44} mode using the impure samples.

In order to evaluate the TOEC we grouped the resultant equations in the manner indicated above. The six equations governing the first five constants in Table III were put into a least-squares program in order to determine the "best" values for the TOEC. Two different weighting schemes were used. The first scheme was an unweighted substitution while the second scheme was to weight inversely the different lines according to the experimental scatter of the points from the best straight line in each individual run. The results along with the weighting scheme are shown in Table IV. The numbers in the parentheses in the weighting column refer to the lines in Table II. The "errors" refer to the self-consistency of the measurements. We see that this consistency is improved somewhat by weighting as in the second line in Table IV. A similar weighting scheme was used for the constants C_{133} and C_{333} giving the values (in units of 10^{12} dyn/cm^2) $C_{133}=-3.53\pm0.11$; $C_{333}=-7.23\pm0.20$. The constants C_{144}, C_{155}, C_{344} are obtained from the solution of three simultaneous equations in these three unknowns. The results are (in units of 10^{12} dyn/cm^2) $C_{144}=-0.10\pm0.10$; $C_{155}=+2.53\pm0.50$; $C_{344}=-4.43\pm0.40$.

Our final values of the TOEC of zinc are given in Table V, along with the hydrostatic-pressure derivatives of the second-order elastic constants which are calculated, via the formulation of Thurston and Brugger,[7] from the TOEC. The errors represent an indication of our confidence in the final values.

TABLE V. TOEC of Zn and hydrostatic pressure derivatives of the second-order elastic constants. [C_{ijk} in units of 10^{12} dyn/cm^2, with $\partial C_{11}/\partial P=7.52$; $\partial C_{33}/\partial P=7.32$; $\partial\frac{1}{2}[C_{11}-C_{12}]/\partial P=1.48$; $\partial C_{44}/\partial P=4.02$.]

$C_{111}=-17.6\pm1.5$	$C_{123}=-2.1\pm0.6$	$C_{133}=-3.5\pm0.1$
$C_{112}=-\ 4.4\pm1.1$	$C_{113}=-2.7\pm0.3$	$C_{133}=-7.2\pm0.2$
$C_{222}=-24.1\pm2.6$	$C_{144}=-0.1\pm0.1$	$C_{155}=+2.5\pm0.5$
		$C_{344}=-4.4\pm0.4$

DISCUSSION AND CONCLUSIONS

(1) The complete set of ten third-order elastic constants of zinc was determined from measurements of the hydrostatic and uniaxial stress dependence of ultrasonic velocity. In the course of these measurements the temperature and pressure derivatives of the second-order elastic constants have been obtained and are reported.

(2) From the values of the second-order elastic constants and the third-order elastic constants determined in the present study the Grüneisen parameter γ for zinc wase valuated. The room-temperature value of the volume thermal-expansion coefficient, α, was then calculated using this Grüneisen parameter. The results were found to agree well with the experimental value of the volume thermal-expansion coefficient, but not with the tensor components of the linear-expansion coefficient.

Values of γ were calculated from the expression for the generalized-mode Grüneisen parameter[9]

$$\gamma_i{}^{pq}=-(1/2W_i)[2W_iU_pU_q+(C_{pqmn}+C_{pqmunv}U_uU_v)N_mN_n], \quad (4)$$

where

$$W_i=C_{munv}N_mN_nU_uU_v, \quad (5)$$

and summation over repeated indices is implied.

For the purpose of relating the thermal expansion coefficient with the Grüneisen parameter the following expression was used:

$$C_{pqij}\alpha_{ij}=\rho_0C_v\bar{\gamma}^{pq} \quad (6)$$

[the derivation of Eq. (6) is given in the Appendix], where, for zinc,

$$\alpha_{ij}=\begin{vmatrix}\alpha_{11} & 0 & 0\\ 0 & \alpha_{11} & 0\\ 0 & 0 & \alpha_{33}\end{vmatrix}.$$

α_{11} and α_{33} are the thermal-expansion coefficients normal and parallel to the axis of sixfold symmetry, respectively. It follows that

$$\alpha_{\text{vol}}=2\alpha_{11}+\alpha_{33}.$$

The average values of γ were calculated (on a computer) over 238 equally spaced points on $\frac{1}{12}$ of the Debye sphere, following the general method outlined by

---

[9] Y. Hiki, J. F. Thomas, and A. V. Granato, Phys. Rev. **153**, 764 (1967).

Quimby and Sutton.[10]

$$\bar{\gamma}^{11}=\bar{\gamma}^{22}=1.192;\quad \bar{\gamma}^{33}=2.812.$$

The volume-expansion coefficient is then calculated from

$$\alpha_{\text{vol}}=\rho_0 C_v \frac{[2(C_{33}-C_{13})\bar{\gamma}^{11}+(C_{11}+C_{12}-2C_{13})\bar{\gamma}^{33}]}{(C_{11}+C_{12})C_{33}-2C_{13}^2},$$

where C_v is the specific heat and ρ_0 is the density. We obtain

$$\alpha_{\text{vol}}=8.8\times 10^{-5}.$$

This number is to be compared with the experimental value[6] of 9.59×10^{-5}.

APPENDIX

We use the following procedure to derive Eq. (6). The free energy F per unit volume of a system of harmonic oscillators can be written in the form

$$F=F_0(\eta)+\rho_0 kT\sum_i \ln(1-e^{-\hbar\omega_i/kT}),$$

where F_0 is independent of temperature, η is the strain, ρ_0 is the density in the undeformed state, ω_i is the circular frequency of the ith mode, k, T, and $\hbar$ have the usual meaning. The stress tensor t_{pq} is given by

$$\begin{aligned}t_{pq}&=\rho_0(\partial F/\partial\eta_{pq})_T\\&=\rho_0\partial F_0/\partial\eta_{pq}+\rho_0 kT\sum_i (1-e^{-\hbar\omega_i/kT})^{-1}\\&\quad\times(-e^{-\hbar\omega_i/kT})(-\hbar/kT)(\partial\omega_i/\partial\eta_{pq}),\end{aligned}\qquad\text{(A1)}$$

which can be rewritten as

$$\begin{aligned}t_{pq}&=\rho_0\partial F_0/\partial\eta_{pq}-\rho_0\sum_i \hbar\omega_i(e^{h\omega_i/kT}-1)^{-1}\\&\quad\times(\omega_i^{-1}\partial\omega_i/\partial\eta_{pq})=t_0-\rho_0\sum_i \langle E_i\rangle\gamma_i^{pq},\end{aligned}\qquad\text{(A2)}$$

where we define

$$\gamma_i^{pq}\equiv(-\omega_i^{-1}\partial\omega_i/\partial\eta_{pq}).\qquad\text{(A3)}$$

Differentiation of t_{pq} with respect to temperature yields

$$\begin{aligned}(\partial t_{pq}/\partial T)_\eta&=-\rho_0\sum_i (\partial\langle E_i\rangle/\partial T)\gamma_i^{pq}\\&=-C_\eta\rho_0\sum_i \gamma_i^{pq}/\sum_i 1=-\rho_0 C\bar{\gamma}^{pq},\end{aligned}\qquad\text{(A4)}$$

where C_η is the specific heat (at constant strain) and $\bar{\gamma}^{pq}$ is the Grüneisen parameter averaged over the Debye sphere.

Further manipulation yields

$$\begin{aligned}(\partial t_{pq}/\partial T)_\eta&=-(\partial t_{pq}/\partial\eta_{ij})(\partial\eta_{ij}/\partial T)_{t_{pq}}\\&=-C_{pqij}{}^T(\partial\eta_{ij}/\partial T)_{t_{pq}},\end{aligned}\qquad\text{(A5)}$$

and with the relation

$$\alpha_{ij}=\partial\eta_{ij}/\partial T\qquad\text{(A6)}$$

we obtain, by using Eqs. (9)–(11),

$$C_{pqij}{}^T\alpha_{ij}=\rho_0 C_\eta\bar{\gamma}^{pq},$$

which is Eq. (6) used in the text, with $C_\eta=C_v$ at zero strain.

---

[10] S. L. Quimby and P. M. Sutton, Phys. Rev. 91, 1122 (1953).